Discussion on 3d Ising spectrum

based on:

Simmons-Duffin 1612.08471

Komargodski, Simmons-Duffin 1603.04444

Simmons-Duffin, S.R., Zan 1612.02436

Behan, Rastelli, S.R., Zan 1703.03430
1703.05325

$$\Delta_\sigma = 0.5181489(10), \qquad f_{\sigma\sigma\epsilon} = 1.0518537(41),$$
$$\Delta_\epsilon = 1.412625(10), \qquad f_{\epsilon\epsilon\epsilon} = 1.532435(19).$$

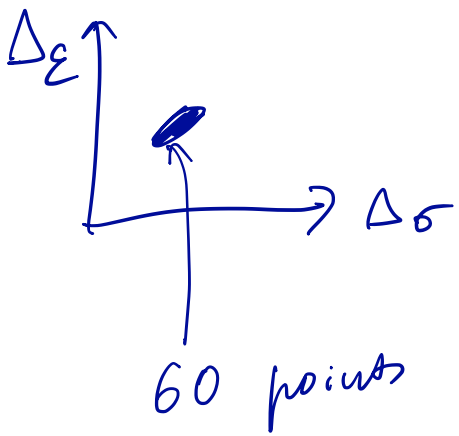

$\sigma\sigma$ $\sigma\sigma$
$\sigma\sigma$ $\varepsilon\varepsilon$
$\varepsilon\varepsilon$ $\varepsilon\varepsilon$

$\sigma \times \sigma \supset O_+$

$\varepsilon \times \varepsilon \supset O_+$

$\sigma \times \varepsilon \supset O_-$

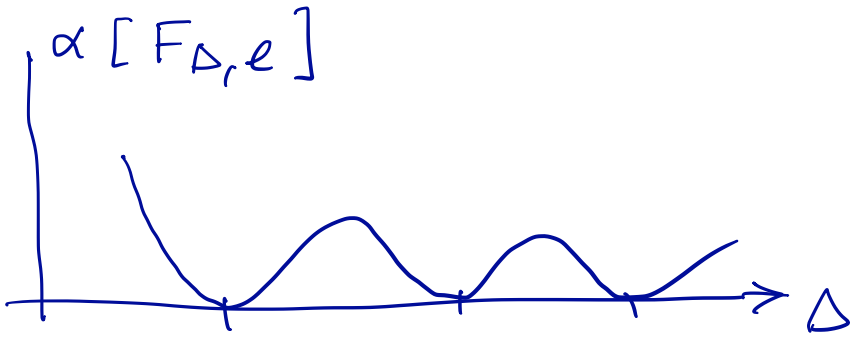

→ - spectrum
- OPE coeffs.

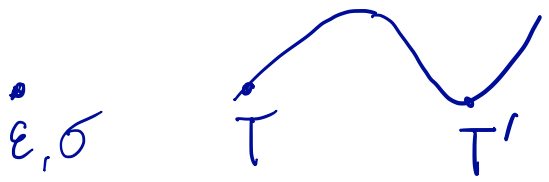
ε, σ
T
T'

$$\Delta_\sigma = 0.5181489(10), \qquad f_{\sigma\sigma\epsilon} = 1.0518537(41),$$
$$\Delta_\epsilon = 1.412625(10), \qquad f_{\epsilon\epsilon\epsilon} = 1.532435(19).$$

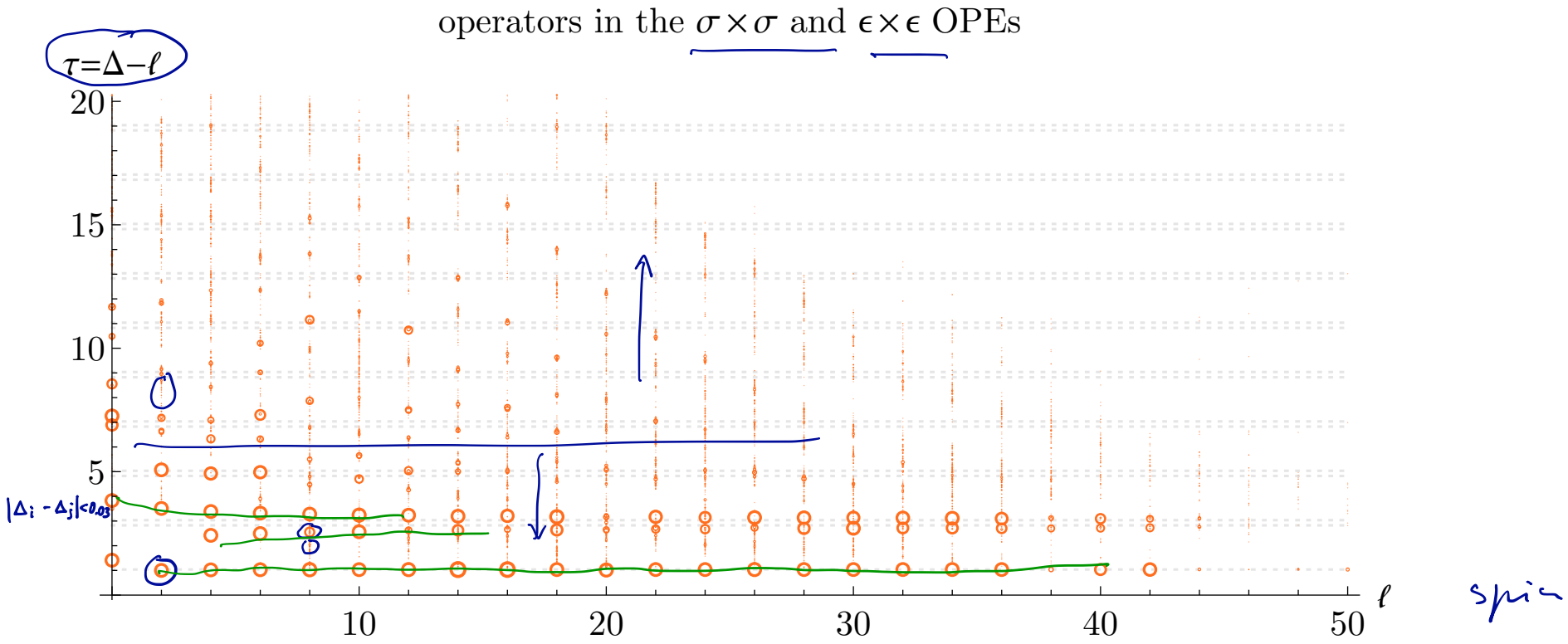

Figure 1: Estimates of $\mathbb{Z}_2$-even operators in the 3d Ising model. Larger circles represent "stable" operators whose dimensions and OPE coefficients have small errors in our computation. We plot the twist $\Delta - \ell$ versus spin ℓ. The grey dashed lines are $\tau = 2\Delta_\sigma + 2n$ and $\tau = 2\Delta_\epsilon + 2n$ for nonnegative integer n.

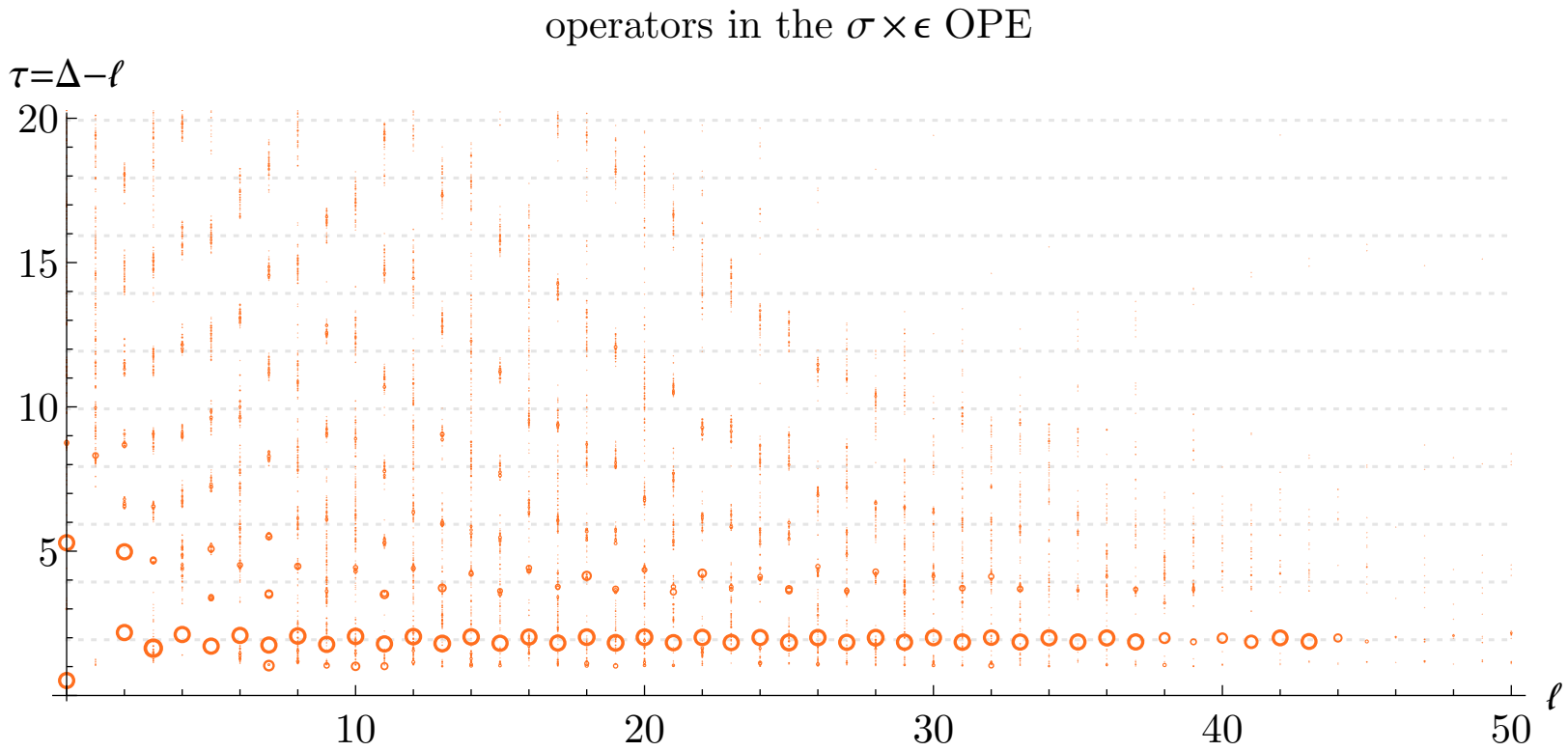

Figure 2: Estimates of $\mathbb{Z}_2$-odd operators in the 3d Ising model. Larger circles represent "stable" operators. We plot the twist $\Delta - \ell$ versus spin ℓ. The grey dashed lines are $\tau = \Delta_\sigma + \Delta_\epsilon + 2n$ for nonnegative integer n.

$\tau = \Delta - \ell$

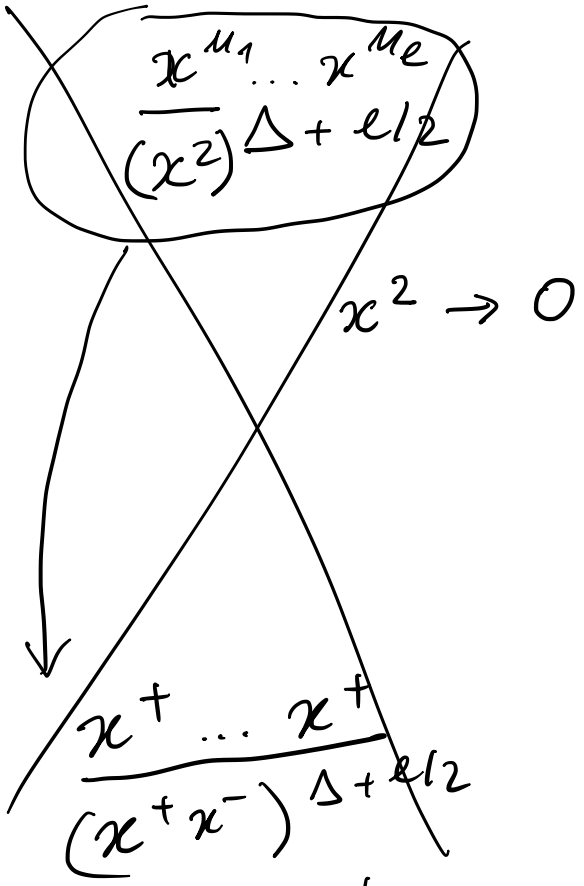

Eucl.

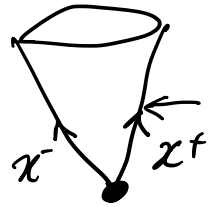

$x^+ = \text{const}$

$x^- \to 0$

$x^2 = x^+ \cdot x^-$

$x^+ = x + t$

$x^- = x - t$

$$C(x) = \frac{x^{\mu_1} \dots x^{\mu_\ell}}{(x^2)^{\ell/2}} \cdot (x^2)^{\Delta/2} \sim (x^-)^{\Delta - \ell}$$

$x^- \to 0$

$C(x) \cdot O_{\Delta, \ell}(0)$

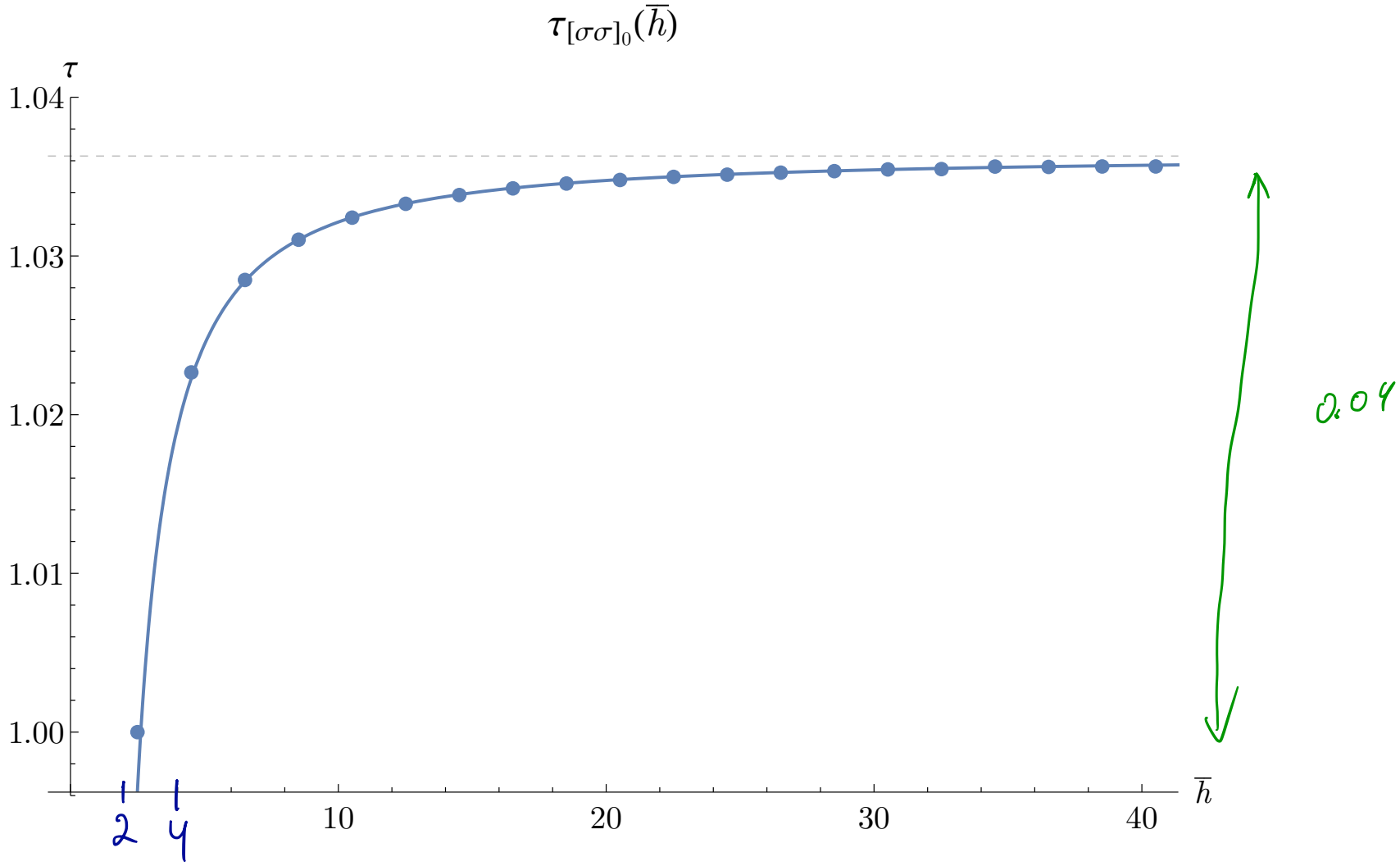

Figure 7: A comparison between the analytical prediction (6.5) (blue curve) and numerical data (blue dots) for $\tau_{[\sigma\sigma]_0}$. The two agree with accuracy 3×10^{-3} and 5×10^{-4} for spins $\ell = 2, 4$, respectively, and $\sim 5 \times 10^{-5}$ for $\ell > 4$. The grey dashed line is the asymptotic value $\tau = 2\Delta_\sigma$. The curve (2.3) from [1] looks essentially the same.

"Theorem" O_1 Δ_1, O_2 Δ_2

$d > 2$ dims.

$[O_1 O_2]_{\ell, n \in \mathbb{N}}$.

$\ell \geq \ell_0 \quad \forall n \in \mathbb{Z}_{\geq 0}$

$\tau\left([O_1 O_2]_{\ell, n}\right) \xrightarrow[\ell \to \infty]{} \Delta_1 + \Delta_2 + 2n$

GFF O_1 O_2

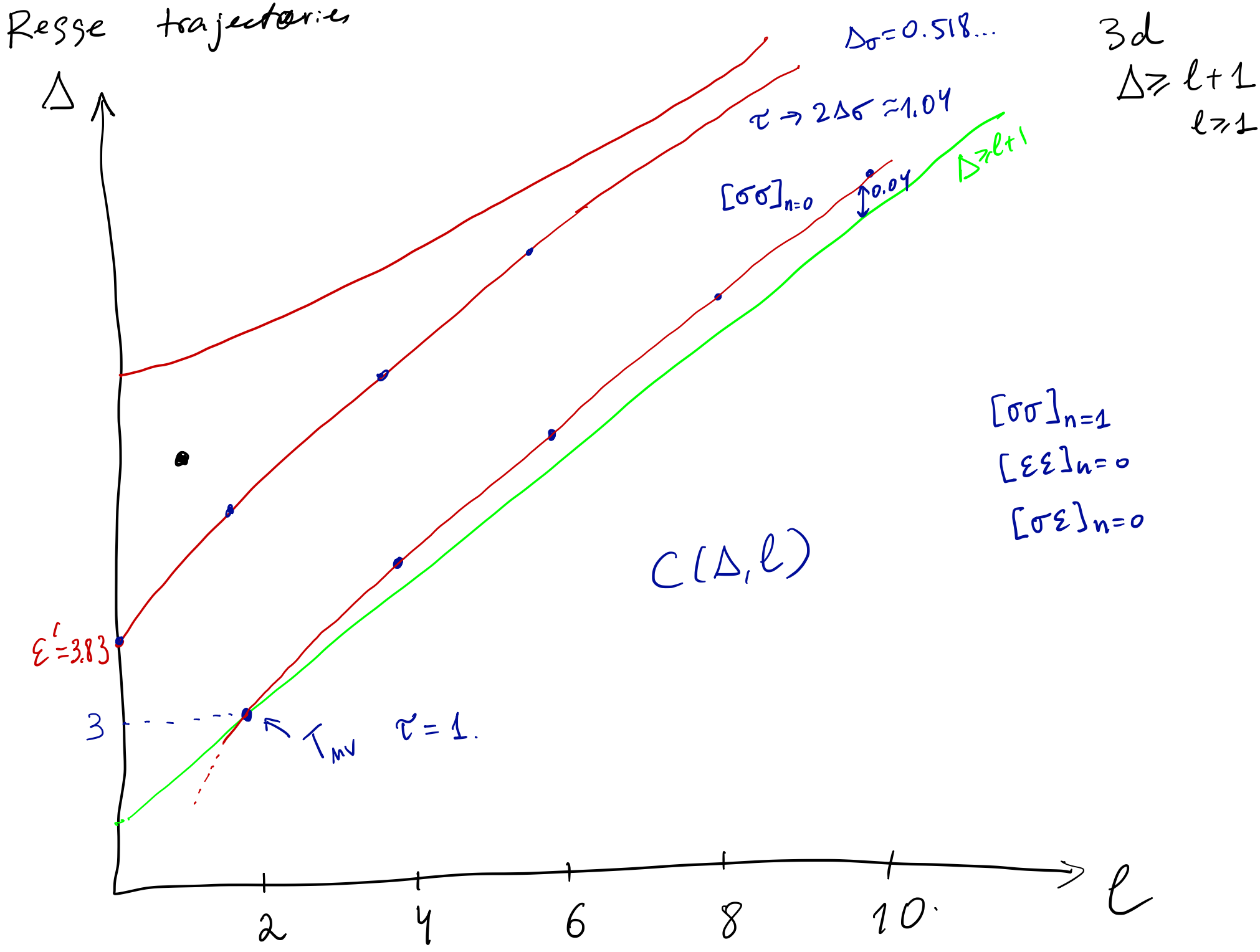
Regge trajectories
$\Delta_\sigma = 0.518\ldots$
3d
$\Delta \geq \ell + 1$
$\ell \geq 1$
$\tau \to 2\Delta_\sigma \simeq 1.04$
$[\sigma\sigma]_{n=0}$
0.04
$\Delta \geq \ell + 1$
$[\sigma\sigma]_{n=1}$
$[\varepsilon\varepsilon]_{n=0}$
$[\sigma\varepsilon]_{n=0}$
$C(\Delta, \ell)$
Δ
ℓ
$\varepsilon' = 3.83$
3
T_{MV} $\tau = 1.$
2
4
6
8
10.

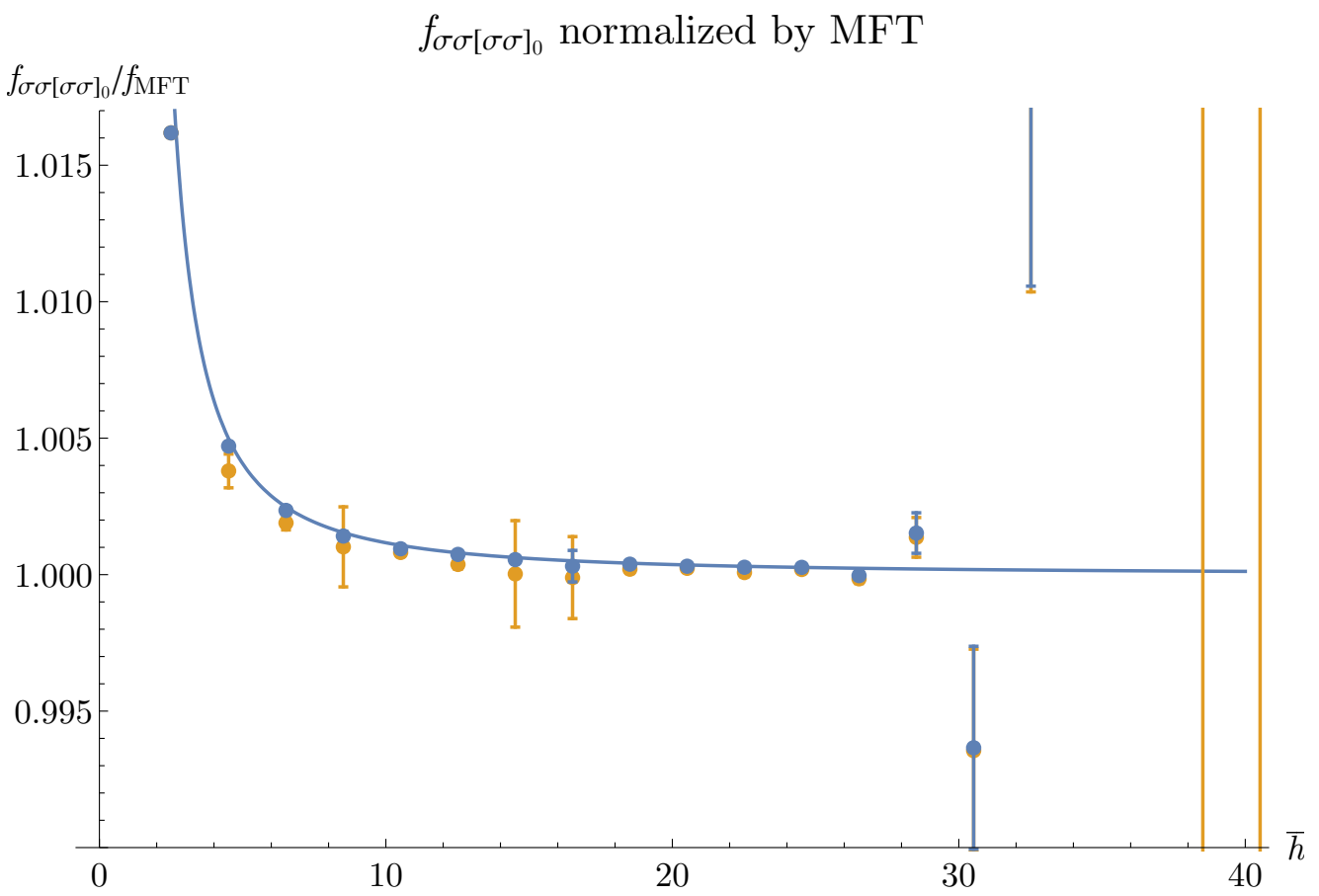

Figure 9: A comparison between the analytical prediction (6.6) and numerics for $f_{\sigma\sigma[\sigma\sigma]_0}$, both normalized by dividing by the Mean Field Theory OPE coefficients $f_{\text{MFT}} = (2S_{-2h_\sigma}(\overline{h}))^{1/2}$. We show two sets of numerical data. The orange series gives the OPE coefficients of the operators $\mathcal{O}_\ell$ with twist closest to $\tau_{[\sigma\sigma]_0}$ for each spin ℓ. The blue series combines the contributions of $\mathcal{O}_\ell$ and spurious higher-spin currents J_ℓ into $(f^2_{\sigma\sigma\mathcal{O}_\ell} + f^2_{\sigma\sigma J_\ell})^{1/2}$. The latter quantities have smaller errors and better match the analytical prediction. The fact that the errors shrink after this modification supports the idea that the correct OPE coefficient is being shared between the real operators $\mathcal{O}_\ell$ and "fake" operators J_ℓ.

In practice

$\langle \sigma\sigma\sigma\sigma \rangle$ $\overset{2d}{=}$ $\sqrt[4]{1-z}$

$\langle \sigma\sigma\varepsilon\varepsilon \rangle$

$\langle \varepsilon\varepsilon\varepsilon\varepsilon \rangle$

Perturbation of 3d Ising CFT — weakly relevant

1) $CFT_1 + \dots + CFT_n + \int \sum_{i,j=1,\, i\neq j}^{n} \varepsilon_i \cdot \varepsilon_j \, d^3x$

$\mu \left(\sum_{i=1}^{n} \varepsilon_i \right)$

$[\varepsilon] = 1.41\dots$

$n = 2$

$O(2)$ 3d

$S^n \times (\mathbb{Z}_2)^n$

- $f_{\varepsilon\varepsilon\varepsilon}$
- $\langle \varepsilon\varepsilon\varepsilon\varepsilon \rangle$

Komargodski, Simmons-Duffin

LRI

2) $CFT + MFT(\chi) + \int \chi \cdot \sigma \, d^3x$

$3 - \Delta_\sigma - \varepsilon$

weakly relevant

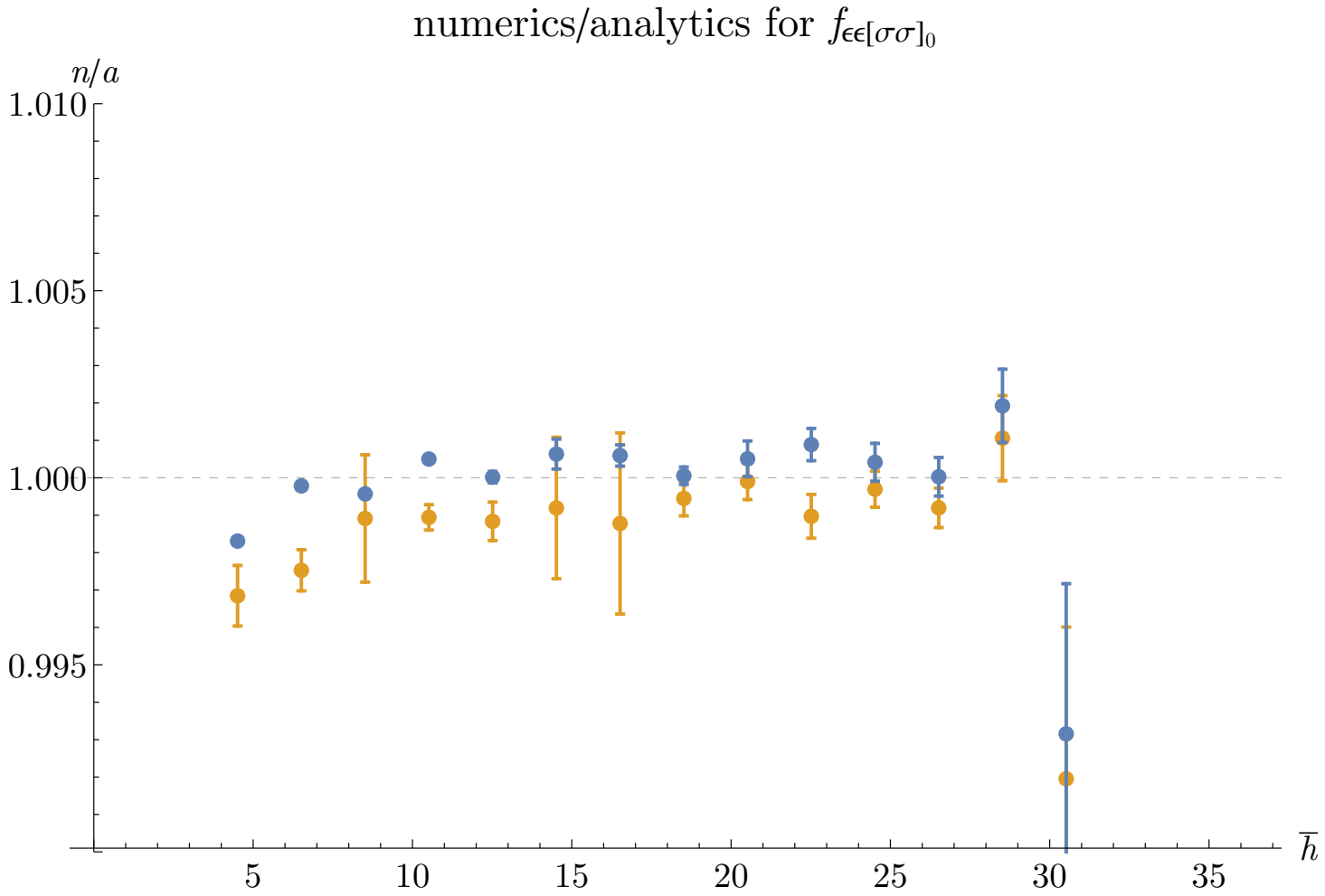

Figure 12: Ratios n/a of numerical results to the analytical prediction (6.1, 6.31) for $f_{\epsilon\epsilon[\sigma\sigma]_0}$. (One must multiply by the Jacobian $\frac{\partial\overline{h}}{\partial\ell}$ to relate $f_{\epsilon\epsilon[\sigma\sigma]_0}$ to $\lambda_{\epsilon\epsilon[\sigma\sigma]_0}$.) As in figure 9, we show two sets of numerical data. The orange series are the raw OPE coefficients $f_{\epsilon\epsilon\mathcal{O}_\ell}$ of operators with twists $\tau_{[\sigma\sigma]_0}$. The blue series are the improved coefficients $(f^2_{\epsilon\epsilon\mathcal{O}_\ell} + f^2_{\epsilon\epsilon J_\ell})^{1/2}$ discussed in section 6.1.

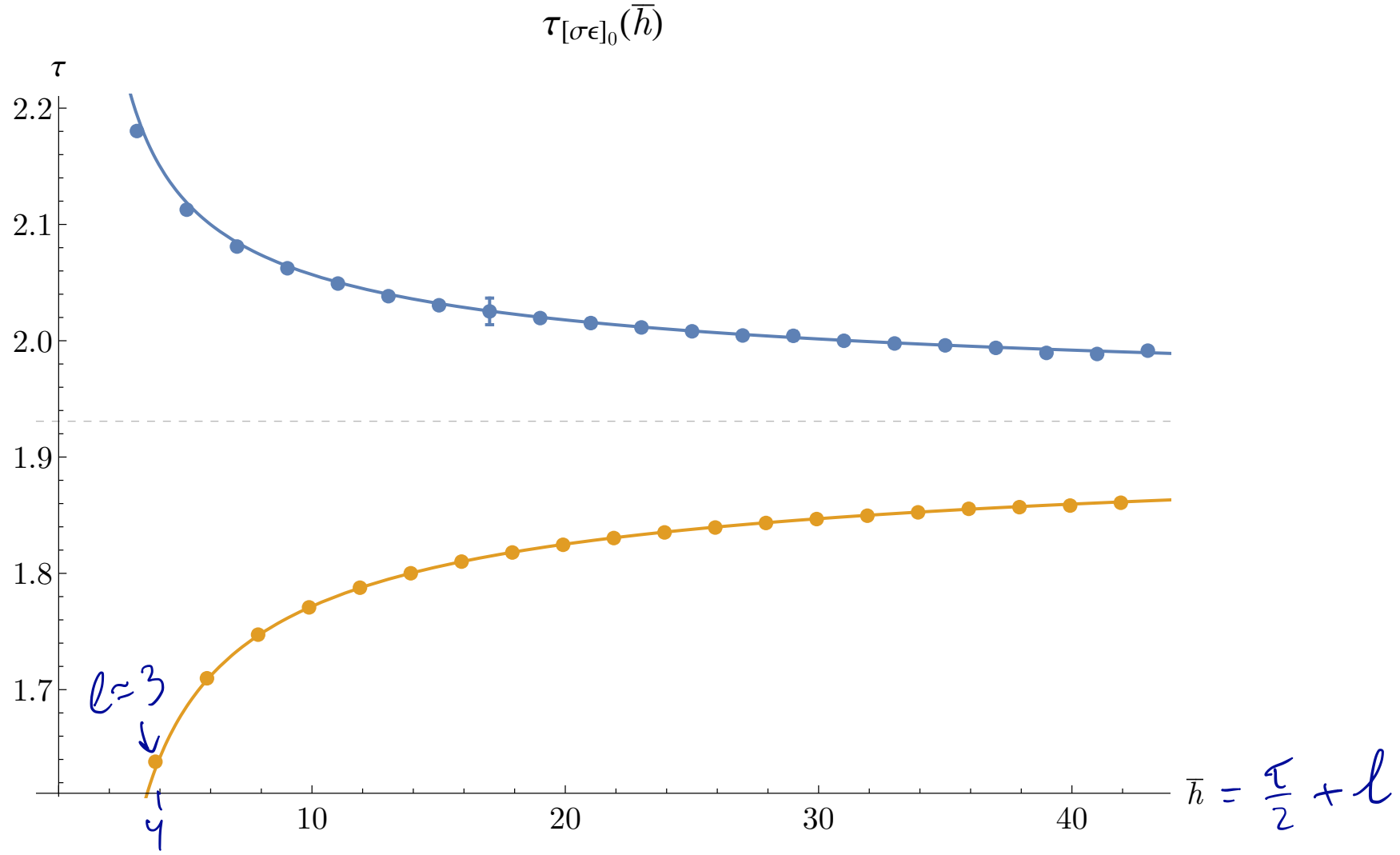

Figure 13: Comparison between numerical data and the analytical prediction (6.33, 6.34) for $\tau_{[\sigma\epsilon]_0}$. The blue curve and points correspond to even-spin operators and the orange curve and points correspond to odd-spin operators. The dashed line is the asymptotic value $\tau = \Delta_\sigma + \Delta_\epsilon$.

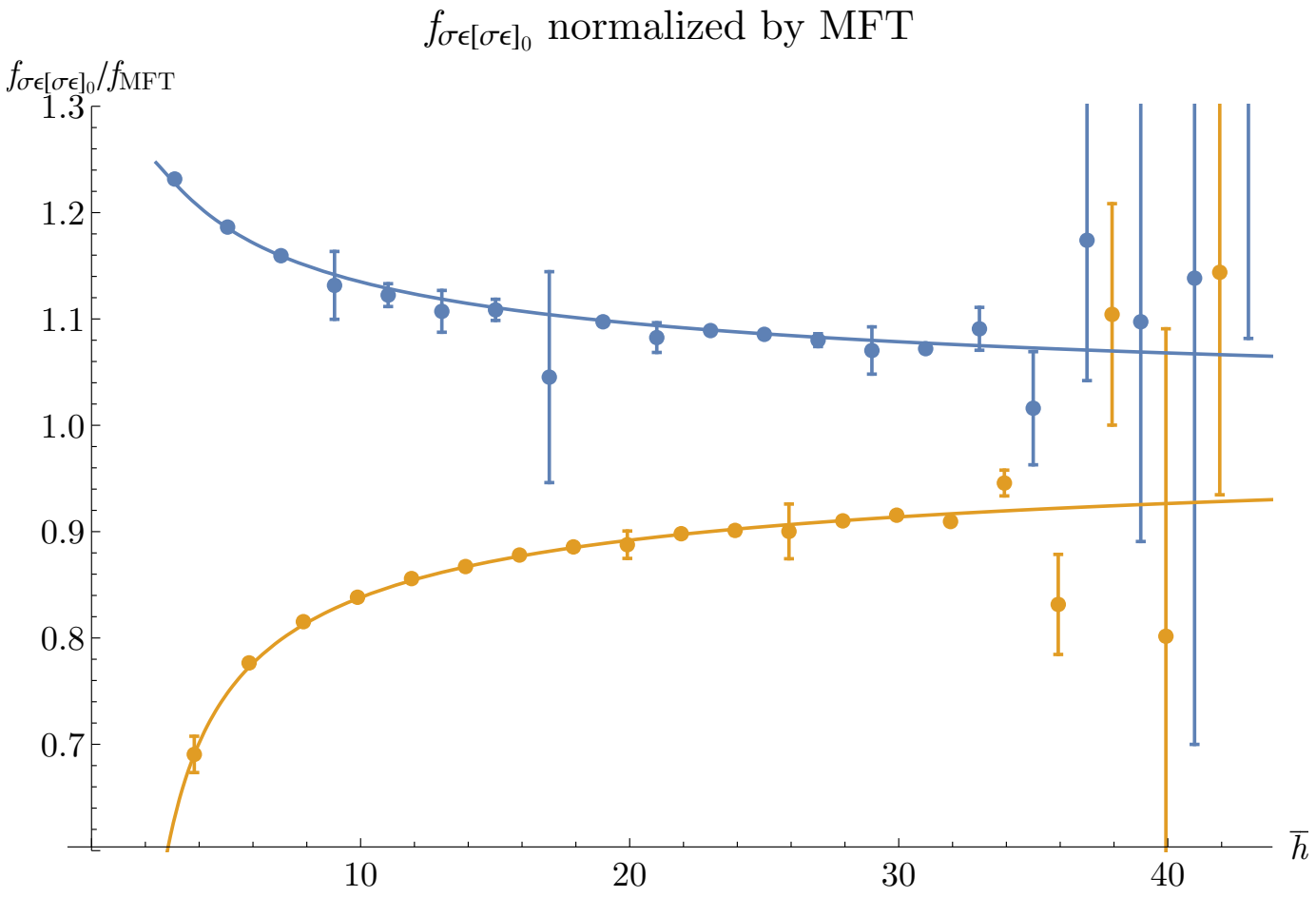

Figure 14: Comparison between numerical data and the analytical prediction (6.33) for $f_{\sigma\epsilon[\sigma\epsilon]_0}$, both divided by the Mean Field Theory OPE coefficients $f_{\text{MFT}} = S^{h_{\sigma\epsilon},h_{\epsilon\sigma}}_{-h_\sigma-h_\epsilon}(\overline{h})^{1/2}$. The blue curve and points correspond to even-spin operators and the orange curve and points correspond to odd-spin operators.

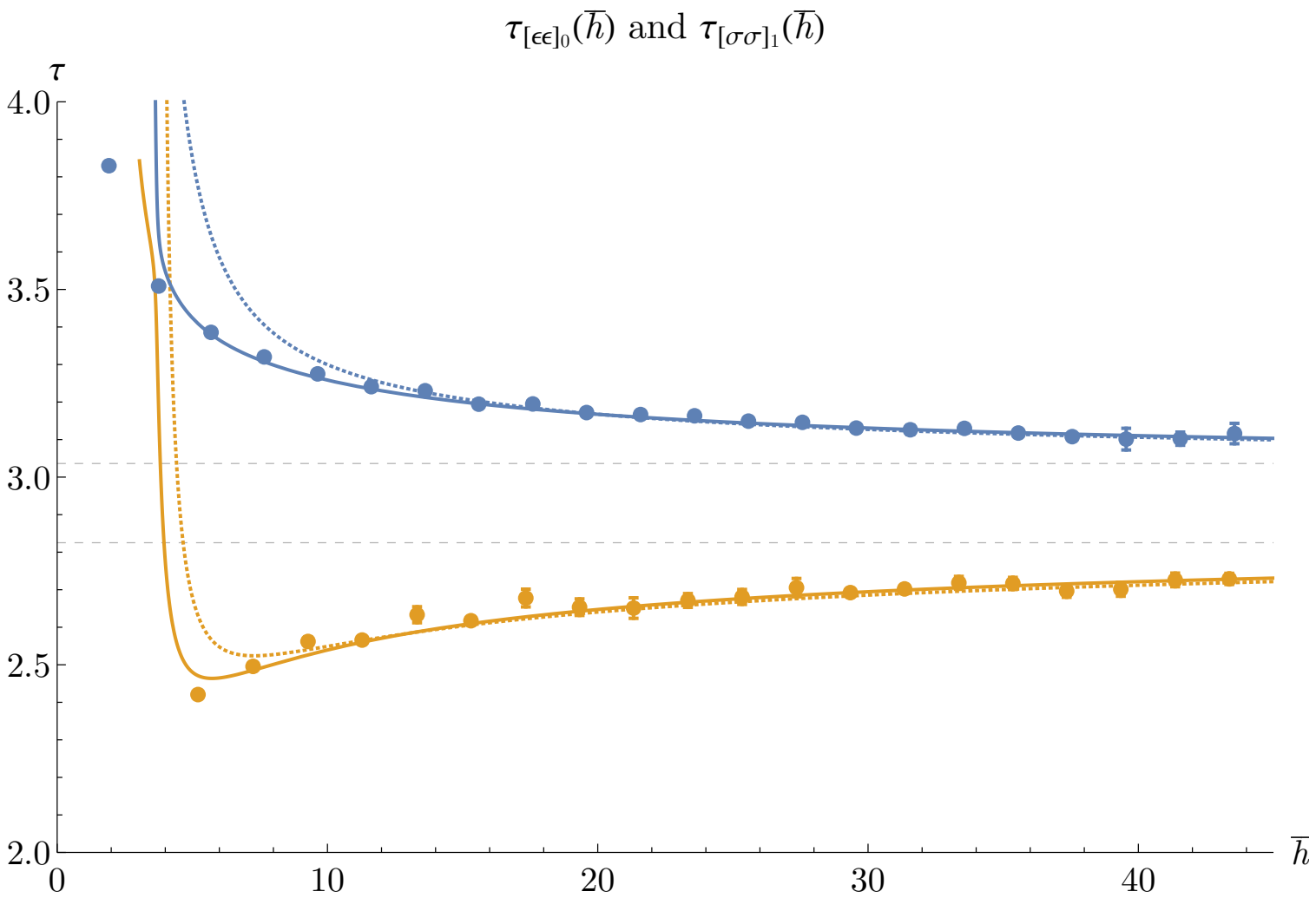

Figure 17: Comparison between numerical data and analytical predictions for $\tau_{[\sigma\sigma]_1}$ (blue) and $\tau_{[\epsilon\epsilon]_0}$ (orange). Solid lines correspond to $\overline{y}_0 = 0.1$, and dotted lines correspond to $\overline{y}_0 = 0.02$. The orange curve ramps up sharply (moving from right to left) near $\overline{h} \approx 3.4$ because $M(\overline{y}_0, \overline{h})$ becomes degenerate there. This coincides with the lower end of the family $[\epsilon\epsilon]_0$.

$\mathcal{O}$	$\mathbb{Z}_2$	ℓ	Δ	$\tau = \Delta - \ell$	$f_{\sigma\sigma\mathcal{O}}$	$f_{\epsilon\epsilon\mathcal{O}}$
ϵ	$+$	0	1.412625**(10)**	1.412625**(10)**	1.0518537**(41)**	1.532435**(19)**
ϵ'	$+$	0	3.82968(23)	3.82968(23)	0.053012(55)	1.5360(16)
	$+$	0	6.8956(43)	6.8956(43)	0.0007338(31)	0.1279(17)
	$+$	0	7.2535(51)	7.2535(51)	0.000162(12)	0.1874(31)
$T_{\mu\nu}$	$+$	2	3	1	0.32613776(45)	0.8891471(40)
$T'_{\mu\nu}$	$+$	2	5.50915(44)	3.50915(44)	0.0105745(42)	0.69023(49)
	$+$	2	7.0758(58)	5.0758(58)	0.0004773(62)	0.21882(73)
$C_{\mu\nu\rho\sigma}$	$+$	4	5.022665(28)	1.022665(28)	0.069076(43)	0.24792(20)
	$+$	4	6.42065(64)	2.42065(64)	0.0019552(12)	$-0.110247(54)$
	$+$	4	7.38568(28)	3.38568(28)	0.00237745(44)	0.22975(10)
	$+$	6	7.028488(16)	1.028488(16)	0.0157416(41)	0.066136(36)
$\mathcal{O}$	$\mathbb{Z}_2$	ℓ	Δ	$\tau = \Delta - \ell$	$f_{\sigma\epsilon\mathcal{O}}$	-
σ	$-$	0	0.5181489**(10)**	0.5181489**(10)**	1.0518537**(41)**	
σ'	$-$	0	5.2906(11)	5.2906(11)	0.057235(20)	
	$-$	2	4.180305(18)	2.180305(18)	0.38915941(81)	
	$-$	2	6.9873(53)	4.9873(53)	0.017413(73)	
	$-$	3	4.63804(88)	1.63804(88)	0.1385(34)	
	$-$	4	6.112674(19)	2.112674(19)	0.1077052(16)	
	$-$	5	6.709778(27)	1.709778(27)	0.04191549(88)	

Table 2: Stable operators with dimensions $\Delta \leq 8$. The leftmost column shows the names of the operators from [20]. Errors in bold are rigorous. All other errors are non-rigorous. Because we have chosen different conventions for conformal blocks, our normalization of OPE coefficients differs from those in [20, 68] by (A.17).

$\mathbb{Z}_2$	ℓ	Δ	$\tau = \Delta - \ell$	$f_{\sigma\sigma\mathcal{O}}$	$f_{\epsilon\epsilon\mathcal{O}}$
+	2	3	1	0.32613776(45)	0.8891471(40)
+	4	5.022665(28)	1.022665(28)	0.069076(43)	0.24792(20)
+	6	7.028488(16)	1.028488(16)	0.0157416(41)	0.066136(36)
+	8	9.031023(30)	1.031023(30)	0.0036850(54)	0.017318(30)
+	10	11.0324141(99)	1.0324141(99)	0.00087562(13)	0.0044811(15)
+	12	13.033286(12)	1.033286(12)	0.000209920(37)	0.00115174(59)
+	14	15.033838(15)	1.033838(15)	0.000050650(99)	0.00029484(56)
+	16	17.034258(34)	1.034258(34)	0.000012280(18)	0.00007517(18)
+	18	19.034564(12)	1.034564(12)	$2.98935(46) \cdot 10^{-6}$	0.0000191408(89)
+	20	21.0347884(84)	1.0347884(84)	$7.2954(10) \cdot 10^{-7}$	$4.8632(23) \cdot 10^{-6}$
+	22	23.034983(11)	1.034983(11)	$1.78412(27) \cdot 10^{-7}$	$1.23201(72) \cdot 10^{-6}$
+	24	25.035122(11)	1.035122(11)	$4.37261(60) \cdot 10^{-8}$	$3.1223(15) \cdot 10^{-7}$
+	26	27.035249(11)	1.035249(11)	$1.07287(18) \cdot 10^{-8}$	$7.8948(42) \cdot 10^{-8}$
+	28	29.035344(19)	1.035344(19)	$2.6409(19) \cdot 10^{-9}$	$1.9992(23) \cdot 10^{-8}$
+	30	31.035452(16)	1.035452(16)	$6.447(24) \cdot 10^{-10}$	$5.003(20) \cdot 10^{-9}$
+	32	33.035473(28)	1.035473(28)	$1.640(25) \cdot 10^{-10}$	$1.308(21) \cdot 10^{-9}$
+	34	35.035632(67)	1.035632(67)	$3.58(22) \cdot 10^{-11}$	$2.90(19) \cdot 10^{-10}$
+	36	37.035610(41)	1.035610(41)	$1.15(13) \cdot 10^{-11}$	$9.6(11) \cdot 10^{-11}$
+	38	39.035638(58)	1.035638(58)	$2.26(71) \cdot 10^{-12}$	$1.93(60) \cdot 10^{-11}$
+	40	41.03564(13)	1.03564(13)	$7.3(15) \cdot 10^{-13}$	$6.3(13) \cdot 10^{-12}$

Table 3: Operators in the family $[\sigma\sigma]_0$. The first line is the stress tensor $T_{\mu\nu}$.

$\mathbb{Z}_2$	ℓ	Δ	$\tau = \Delta - \ell$	$f_{\sigma\sigma\mathcal{O}}$	$f_{\epsilon\epsilon\mathcal{O}}$
+	4	6.42065(64)	2.42065(64)	0.0019552(12)	−0.110247(54)
+	6	8.4957(75)	2.4957(75)	0.000472(49)	−0.0431(48)
+	8	10.562(12)	2.562(12)	0.0001084(69)	−0.0139(11)
+	10	12.5659(57)	2.5659(57)	0.00002598(39)	−0.004437(62)
+	12	14.633(21)	2.633(21)	$6.10(33) \cdot 10^{-6}$	−0.001224(60)
+	14	16.6174(75)	2.6174(75)	$1.417(34) \cdot 10^{-6}$	−0.0003791(54)
+	16	18.678(24)	2.678(24)	$3.547(59) \cdot 10^{-7}$	−0.0000972(64)
+	18	20.654(22)	2.654(22)	$7.99(90) \cdot 10^{-8}$	−0.0000284(26)
+	20	22.651(27)	2.651(27)	$1.83(13) \cdot 10^{-8}$	$-7.58(47) \cdot 10^{-6}$
+	22	24.671(18)	2.671(18)	$4.55(72) \cdot 10^{-9}$	$-2.09(19) \cdot 10^{-6}$
+	24	26.681(20)	2.681(20)	$1.168(29) \cdot 10^{-9}$	$-5.67(17) \cdot 10^{-7}$
+	26	28.706(24)	2.706(24)	$2.81(17) \cdot 10^{-10}$	$-1.49(11) \cdot 10^{-7}$
+	28	30.6923(81)	2.6923(81)	$6.69(36) \cdot 10^{-11}$	$-4.162(88) \cdot 10^{-8}$
+	30	32.702(11)	2.702(11)	$1.62(16) \cdot 10^{-11}$	$-1.066(59) \cdot 10^{-8}$
+	32	34.718(17)	2.718(17)	$4.15(42) \cdot 10^{-12}$	$-2.83(18) \cdot 10^{-9}$
+	34	36.717(16)	2.717(16)	$9.44(77) \cdot 10^{-13}$	$-7.33(59) \cdot 10^{-10}$
+	36	38.697(17)	2.697(17)	$2.40(39) \cdot 10^{-13}$	$-2.12(34) \cdot 10^{-10}$
+	38	40.701(19)	2.701(19)	$5.4(17) \cdot 10^{-14}$	$-5.2(15) \cdot 10^{-11}$
+	40	42.726(18)	2.726(18)	$1.59(49) \cdot 10^{-14}$	$-1.55(48) \cdot 10^{-11}$
+	42	44.729(15)	2.729(15)	$4.2(12) \cdot 10^{-15}$	$-4.4(11) \cdot 10^{-12}$

Table 4: Operators in the family $[\epsilon\epsilon]_0$.

$\mathbb{Z}_2$	ℓ	Δ	$\tau = \Delta - \ell$	$f_{\sigma\sigma\mathcal{O}}$	$f_{\epsilon\epsilon\mathcal{O}}$
+	0	3.82968(23)	3.82968(23)	0.053012(55)	1.5360(16)
+	2	5.50915(44)	3.50915(44)	0.0105745(42)	0.69023(49)
+	4	7.38568(28)	3.38568(28)	0.00237745(44)	0.22975(10)
+	6	9.32032(34)	3.32032(34)	0.00055657(42)	0.06949(11)
+	8	11.2751(24)	3.2751(24)	0.00013251(91)	0.01980(15)
+	10	13.2410(10)	3.2410(10)	0.00003234(15)	0.005459(39)
+	12	15.2301(64)	3.2301(64)	$7.64(14) \cdot 10^{-6}$	0.001538(22)
+	14	17.1944(55)	3.1944(55)	$1.930(46) \cdot 10^{-6}$	0.000386(14)
+	16	19.1950(62)	3.1950(62)	$4.568(72) \cdot 10^{-7}$	0.0001107(16)
+	18	21.1720(23)	3.1720(23)	$1.153(27) \cdot 10^{-7}$	0.00002798(33)
+	20	23.167(10)	3.167(10)	$2.74(11) \cdot 10^{-8}$	$7.45(52) \cdot 10^{-6}$
+	22	25.163(10)	3.163(10)	$6.88(22) \cdot 10^{-9}$	$1.937(51) \cdot 10^{-6}$
+	24	27.1491(82)	3.1491(82)	$1.716(45) \cdot 10^{-9}$	$4.92(42) \cdot 10^{-7}$
+	26	29.1460(53)	3.1460(53)	$4.183(78) \cdot 10^{-10}$	$1.347(62) \cdot 10^{-7}$
+	28	31.1306(52)	3.1306(52)	$1.056(50) \cdot 10^{-10}$	$3.35(10) \cdot 10^{-8}$
+	30	33.126(12)	3.126(12)	$2.54(10) \cdot 10^{-11}$	$8.35(42) \cdot 10^{-9}$
+	32	35.1299(77)	3.1299(77)	$6.71(17) \cdot 10^{-12}$	$2.36(13) \cdot 10^{-9}$
+	34	37.1174(64)	3.1174(64)	$1.39(14) \cdot 10^{-12}$	$4.87(48) \cdot 10^{-10}$
+	36	39.1079(78)	3.1079(78)	$4.84(56) \cdot 10^{-13}$	$1.70(17) \cdot 10^{-10}$
+	38	41.101(29)	3.101(29)	$8.4(28) \cdot 10^{-14}$	$2.5(11) \cdot 10^{-11}$
+	40	43.102(18)	3.102(18)	$2.63(64) \cdot 10^{-14}$	$9.0(26) \cdot 10^{-12}$
+	42	45.116(27)	3.116(27)	$7.9(22) \cdot 10^{-15}$	$3.42(95) \cdot 10^{-12}$

Table 5: Operators in the family $[\sigma\sigma]_1$.

$\mathbb{Z}_2$	ℓ	Δ	$\tau = \Delta - \ell$	$f_{\sigma\epsilon\mathcal{O}}$
–	2	4.180305(18)	2.180305(18)	0.38915941(81)
–	3	4.63804(88)	1.63804(88)	0.1385(34)
–	4	6.112674(19)	2.112674(19)	0.1077052(16)
–	5	6.709778(27)	1.709778(27)	0.04191549(88)
–	6	8.08097(25)	2.08097(25)	0.0286902(80)
–	7	8.747293(56)	1.747293(56)	0.01161255(13)
–	8	10.0623(29)	2.0623(29)	0.00745(21)
–	9	10.77075(36)	1.77075(36)	0.003115(12)
–	10	12.0492(18)	2.0492(18)	0.001940(19)
–	11	12.787668(92)	1.787668(92)	0.000823634(82)
–	12	14.0383(33)	2.0383(33)	0.0004983(88)
–	13	14.80006(51)	1.80006(51)	0.0002150(10)
–	14	16.0305(12)	2.0305(12)	0.0001291(12)
–	15	16.81009(16)	1.81009(16)	0.000055870(15)
–	16	18.025(11)	2.025(11)	0.0000313(30)
–	17	18.81794(18)	1.81794(18)	0.0000144219(91)
–	18	20.01947(94)	2.01947(94)	$8.442(28) \cdot 10^{-6}$
–	19	20.8246(11)	1.8246(11)	$3.690(54) \cdot 10^{-6}$
–	20	22.0152(36)	2.0152(36)	$2.131(28) \cdot 10^{-6}$
–	21	22.83035(11)	1.83035(11)	$9.5120(13) \cdot 10^{-7}$
–	22	24.01143(53)	2.01143(53)	$5.4746(61) \cdot 10^{-7}$
–	23	24.83518(65)	1.83518(65)	$2.428(11) \cdot 10^{-7}$
–	24	26.00809(94)	2.00809(94)	$1.3908(17) \cdot 10^{-7}$
–	25	26.8394(13)	1.8394(13)	$6.16(18) \cdot 10^{-8}$
–	26	28.0045(17)	2.0045(17)	$3.523(20) \cdot 10^{-8}$
–	27	28.84330(31)	1.84330(31)	$1.5809(50) \cdot 10^{-8}$
–	28	30.0042(38)	2.0042(38)	$8.86(18) \cdot 10^{-9}$
–	29	30.84667(23)	1.84667(23)	$4.0311(33) \cdot 10^{-9}$
–	30	31.99996(74)	1.99996(74)	$2.2555(81) \cdot 10^{-9}$
–	31	32.84955(61)	1.84955(61)	$1.0144(28) \cdot 10^{-9}$
–	32	33.9976(28)	1.9976(28)	$5.82(11) \cdot 10^{-10}$
–	33	34.85245(50)	1.85245(50)	$2.669(34) \cdot 10^{-10}$
–	34	35.99600(99)	1.99600(99)	$1.374(72) \cdot 10^{-10}$
–	35	36.85548(90)	1.85548(90)	$5.94(34) \cdot 10^{-11}$
–	36	37.9939(12)	1.9939(12)	$4.02(45) \cdot 10^{-11}$
–	37	38.85691(49)	1.85691(49)	$1.99(19) \cdot 10^{-11}$
–	38	39.9895(17)	1.9895(17)	$9.5(18) \cdot 10^{-12}$
–	39	40.8583(11)	1.8583(11)	$3.7(13) \cdot 10^{-12}$
–	40	41.9886(15)	1.9886(15)	$2.50(96) \cdot 10^{-12}$
–	41	42.8607(14)	1.8607(14)	$1.32(24) \cdot 10^{-12}$
–	42	43.9915(21)	1.9915(21)	$7.9(19) \cdot 10^{-13}$

Table 6: Operators in the family $[\sigma\epsilon]_0$.

$\mathbb{Z}_2$	ℓ	Δ	$\tau = \Delta - \ell$	$f_{\sigma\sigma\mathcal{O}}$	$f_{\epsilon\epsilon\mathcal{O}}$
$+$	0	1.412625**(10)**	1.412625**(10)**	1.0518537**(41)**	1.532435**(19)**
$+$	2	7.0758(58)	5.0758(58)	0.0004773(62)	0.21882(73)
$+$	4	8.9410(99)	4.9410(99)	0.0001173(21)	0.08635(18)
$+$	6	10.975(13)	4.975(13)	0.00002437(59)	0.02775(17)
$+$	0	6.8956(43)	6.8956(43)	0.0007338(31)	0.1279(17)
$+$	0	7.2535(51)	7.2535(51)	0.000162(12)	0.1874(31)
$\mathbb{Z}_2$	ℓ	Δ	$\tau = \Delta - \ell$	$f_{\sigma\epsilon\mathcal{O}}$	-
$-$	0	0.5181489**(10)**	0.5181489**(10)**	1.0518537**(41)**	
$-$	0	5.2906(11)	5.2906(11)	0.057235(20)	
$-$	2	6.9873(53)	4.9873(53)	0.017413(73)	

Table 7: Stable operators not in one of the families $[\sigma\sigma]_0$, $[\epsilon\epsilon]_0$, $[\sigma\sigma]_1$, $[\sigma\epsilon]_0$. Errors in bold are rigorous. All other errors are non-rigorous.

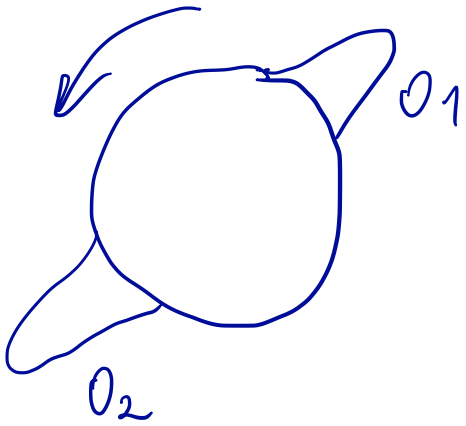
O_1
O_2

Non-gaussianity

$$Q(1,2,3,4) = \frac{\langle\sigma_1\sigma_2\sigma_3\sigma_4\rangle}{\langle\sigma_1\sigma_2\rangle\langle\sigma_3\sigma_4\rangle + \langle\sigma_1\sigma_3\rangle\langle\sigma_2\sigma_4\rangle + \langle\sigma_1\sigma_4\rangle\langle\sigma_2\sigma_3\rangle},$$

$$Q = \frac{g(u,v)}{1 + u^{\Delta_\sigma} + (u/v)^{\Delta_\sigma}} . \quad = \frac{g(z,\bar{z})}{1 + |z|^{2\Delta_\sigma} + (|z|/|1-z|)^{2\Delta_\sigma}} .$$

3 d

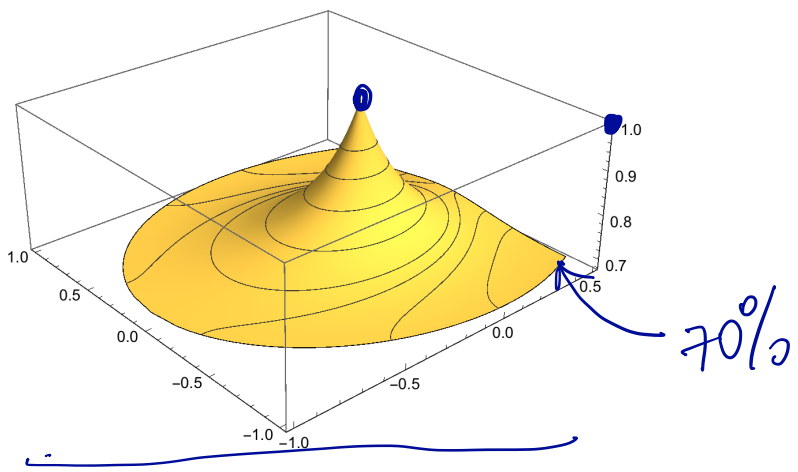

70%

2 d

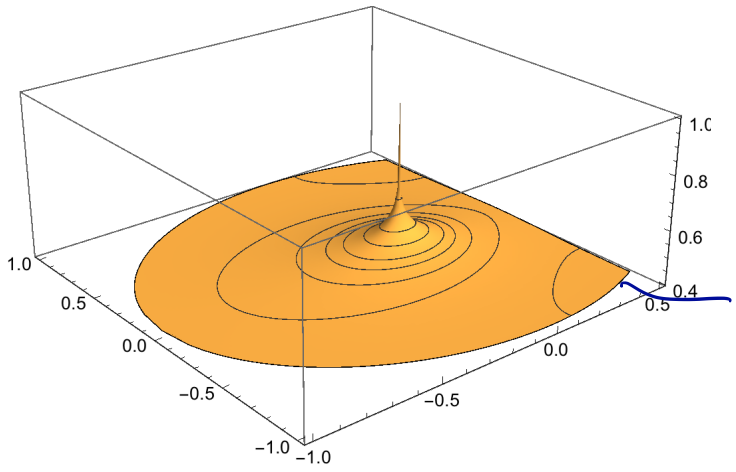

40%